Hindawi
Advances in Civil Engineering
Volume 2022, Article ID 2262289, 17 pages
https://doi.org/10.1155/2022/2262289

Research Article

Investigation on Seismic Response of Long-Span Special Steel Truss Cable-Stayed Bridge

Yong Zeng,[1,2] **Xueqin Li**,[1,2] **and Yutong Zeng**[1,2]

[1]*State Key Laboratory of Mountain Bridge and Tunnel Engineering, Chongqing Jiaotong University, Chongqing, China*
[2]*Mountain Bridge and Materials Engineering Research Center of Ministry of Education, Chongqing Jiaotong University, Chongqing, China*

Correspondence should be addressed to Yong Zeng; yongzeng@cqjtu.edu.cn

Received 30 May 2022; Accepted 2 August 2022; Published 8 October 2022

Academic Editor: Edén Bojórquez

Due to the small self-weight of the steel truss cable-stayed bridge with a single tower and a single cable plane, the torsional stiffness and wind stability of the structure are reduced. The arrangement of the deck type makes the mechanical properties of the cable-stayed bridge more complicated while reducing the cost and increasing the aesthetics. The effects of structural parameter variations and traveling wave effects on the seismic response of this steel truss cable-stayed bridge with a single tower and a single cable plane were investigated by the nonlinear time-history analysis method and nonuniform seismic analysis method. The results show that the displacement of the floating system under seismic action is larger than the other three systems, but its internal force is significantly smaller than the other three systems. The spectral characteristics and the duration of ground shaking have a greater influence on the maximum bending moment values corresponding to the height of the cable tower and the maximum axial force values of the main girder bars corresponding to the length of the bridge under earthquake action. The effect of steel truss girder stiffness parameter variations on structural internal forces of bridges and the effect of traveling wave effects on structural displacements of bridges in specific apparent wave velocity intervals do not exist universally.

1. Introduction

The earthquake has the characteristics of great destructive power, rapid occurrence, and unpredictable source. It is one of the dynamic disasters that bridges may suffer. The steel truss cable-stayed bridge has a beautiful shape, good permeability, good navigability, and flood discharge performance. The single cable deck makes the mechanical properties of cable-stayed bridges complicated and increases the difficulty of construction. The low self-weight of the steel joist beam reduces the torsional stiffness and wind stability of the structure. The single tower increases the risk of wind and earthquake resistance while reducing the cost and increasing the aesthetics. Therefore, a steel truss bridge needs more dynamic analysis than a concrete girder bridge. It is necessary to carry out seismic design for super large bridges [1]. Strong earthquake action may cause very complex damage to a long-span steel truss cable-stayed bridge with a single tower and a single cable plane, so it is of great significance to study its seismic performance.

Many studies on the seismic response of cable-stayed bridges have been conducted around the world [2–5]. Efthymiou et al. [6] considered different sources of spatial variability, i.e., incoherence and traveling wave effect, and carried out the seismic analysis of cable-stayed bridges. Wang et al. [7] carried out the finite element structural analysis of the super long-span cable-stayed bridge and found that the traveling wave effect will increase the seismic damage of the bridge. Li et al. [8] studied the longitudinal seismic susceptibility of a five-span high pier cable-stayed bridge using the susceptibility method. Yan et al. [9] found through experiments that ductile design with plastic hinges on the tower column, i.e., strong pole and weak tower column design, is another effective seismic design strategy, and the residual displacement at the top of the tower column is small even under very strong seismic excitation. Tonyali

et al. [10] studied the random response of cable-stayed bridges under spatially varying ground motions in the case of local soil and variable wave velocity. Ateş et al. [11] investigated the effects of multisupported excitation (MSE) and soil-structure interaction (SSI) on the dynamic characteristics of a cable-stayed bridge built on a cluster of pile foundations. Seeram and Manohar [12] performed a two-dimensional analysis of a cable-stayed bridge under wave loading. Özcebe et al. [13] evaluated the influence of spatial variability of ground motion on spatial scalable structures. Clemente et al. [14] adopted an experimental vibration analysis method to assess the structural health status of a cable-stayed bridge. Zhu et al. [15] investigated the dynamic effects of heavy-duty trains on the seismic response of railroad cable-stayed bridges. Jiantao et al. [16] studied the simplified design method of transverse metal dampers for cable-stayed bridges. Mu et al. [17] investigated the dynamic responses of a cable-stayed bridge under a high-speed train with random track irregularities and a vertical seismic load. Mouloud et al. [18] summarized the influence of spatial variability of ground motion on nonlinear dynamic characteristics of cable-stayed bridges.

The shape of a steel truss cable-stayed bridge with a single tower and a single cable plane is novel and its structure is complex. It is of great practical significance to investigate its structural parameter transformation, traveling wave effect, and seismic vulnerability, and it can provide a reference for the seismic design of similar projects. In this paper, a steel truss cable-stayed bridge with a single tower and a single cable plane is taken as the research object. The seismic response is analyzed by the nonlinear time-history analysis method. Then, three kinds of seismic waves are selected scientifically, and the influence of the traveling wave effect on a steel truss cable-stayed bridge with a single tower and a single cable plane is studied from two aspects of the maximum bending moment and displacement of cable tower and the maximum axial force and displacement of steel truss girder under earthquake action by using nonuniform seismic analysis method.

2. Project Overview of the Bridge

A steel truss cable-stayed bridge with a single tower and a single cable plane is shown in Figure 1. It is the world's first steel truss cable-stayed bridge with a single tower and a single cable plane. The span combination is (88 + 312 + 240 + 80) m. The main girder is arranged as a double-layer steel truss girder, the upper layer is two-way four-lane road traffic, and the lower layer is two-way rail traffic. The double deck adopts an orthotropic deck. The width of the upper orthotropic deck varies from 24 m to 37 m due to functional requirements [19–27]. The tower is shaped like a "Tissot shape" with a height of 182 m and is made of C50 concrete. The distance between the lower anchor and the upper anchor of the stay cable is 16 m and 3.4 m, respectively.

The finite element model of the bridge is built as shown in Figure 2. There are 12806 nodes and 26111 elements in the model. The number of elements is appropriate and the accuracy is enough. The simulation of each component of the bridge is accurate. The materials of the main components of the bridge are shown in Table 1. According to the actual situation of the bridge, we set the support boundary conditions as shown in Table 2. In Table 2, the supports of piers P1, P2, and P3 refer to the supports at the bottom of the piers, while the supports of piers P0 and P4 are not actually modeled in the model, so they refer to the supports at the top of the piers. P1 pier, P2 pier, and P3 pier top are first connected to the superstructure with the common joint, and then the beam end restraint is released to simulate the bearing. The P2 pier top is provided with fixed hinge supports, and the P1 and P3 pier tops are provided with longitudinal living hinge supports. The full-bridge model is based on spatial beam units to simulate the upper and lower chords, diagonal webs, longitudinal beams, rails, piers, and towers, while the diagonal cables are simulated by truss units with the designed initial tensile stresses applied. The upper and lower deck slabs of the bridge are then simulated by the plate unit. During the construction of the model, the overlapping parts of the model, such as the overlapping parts of the upper chord and the deck slab, the middle longitudinal beam and the deck slab, and the tie beam and the deck slab, are deducted and connected by rigid arm units. The stiffness changes of steel truss and stay cables are simulated by changing the elastic modulus of corresponding materials. The nonlinear time-history analysis method is used to analyze the seismic response, and the influence of different structural parameters on the seismic response is observed by transforming a variety of structural parameters. Then, three different seismic waves are input, and the apparent wave velocity of each seismic wave is set between 300 m/s and 7000 m/s.

Figure 1: A steel truss cable-stayed bridge with a single tower and a single cable plane (m).

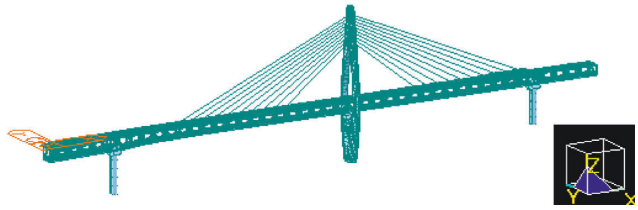

Figure 2: Finite element model of the bridge.

3. Analysis of Theory and Method

3.1. Selection of Seismic Wave and PGA Adjustment

3.1.1. Determination of PGA Adjustment Coefficient. The main span of the bridge is 312 m, belonging to a long bridge. The calculation formula of the maximum horizontal acceleration response spectrum is as follows:

Table 1: Physical properties of main materials.

Position	Material	Elastic modulus, E/GPa	Poisson's ratio	Coefficient of linear expansion/($10^{-50}C^{-1}$)
Tower	C50	34.5	0.2	1.0
Steel truss girder	Q370qD	206.0	0.3	1.2
Stayed cable	Strand1860	195.0	0.3	1.2

$$S_{\max} = 2.25 C_i C_s C_d A. \quad (1)$$

Here, C_i is the bridge importance coefficient, 1.7 for class A bridges under E2 earthquake action, C_s is the site coefficient, 1.0 for the bridge with site type II and seismic fortification of 6, C_d is the damping adjustment coefficient, usually 1.0, A is the peak value of horizontal basic ground motion acceleration, and the seismic fortification intensity is 0.05 g.

The calculation formula of the maximum design acceleration PGA is as follows:

$$\mathrm{PGA} = \frac{S_{\max}}{2.25} = C_i C_s C_d A. \quad (2)$$

The calculation formula of the PGA adjustment coefficient of peak acceleration is as follows:

$$A_e = \frac{\mathrm{PGA}}{P_k}. \quad (3)$$

Among them, P_k is the peak value of the seismic acceleration response spectrum.

Combining formulas (2) and (3), the PGA adjustment coefficient of peak acceleration can be expressed as follows:

$$A_e = \frac{C_i C_s C_d A}{P_k}. \quad (4)$$

3.1.2. The Influence of Structural Parameter Changes. According to the bridge feature, the representative seismic wave is selected and the acceleration peak value is adjusted. The nonlinear time-history analysis of the bridge under E2 earthquake action is carried out, and it is set as the coupling seismic wave along the bridge direction and across the bridge direction.

The El Cento Site 270 Deg seismic wave commonly used in the world is input, and the peak ground acceleration is adjusted by PGA (peak acceleration) adjustment coefficient.

Under El Cento Site 270 Deg seismic wave, the PGA adjustment coefficient is as follows:

$$A_e = \frac{C_i C_s C_d A}{P_k} = \frac{1.7 \times 1.0 \times 1.0 \times 0.05g}{0.3569g} = 0.2382. \quad (5)$$

The time-history function after peak acceleration adjustment is shown in Figure 3.

3.1.3. Traveling Wave Effects. Three kinds of seismic waves with different PGA (peak acceleration), spectrum characteristics, and ground motion duration are selected to explore the influence of the traveling wave effect on long-span steel truss cable-stayed bridge with a single tower and a single cable plane under different seismic waves. The three kinds of seismic waves are the 1979 James RD E1 Centro 220 Deg seismic wave (peak acceleration 0.3673 g and duration 37.68 s), 1994 Northridge Sylmar County Hosp 90 Deg (peak acceleration 0.6047 g and duration 59.98 s), and an artificial wave (peak acceleration 0.1043 g and duration 24.96 s). PGA is different and needs to be adjusted. The amplitude of each seismic wave can be adjusted by the PGA adjustment coefficient.

The PGA adjustment coefficients of three kinds of seismic waves under the action of E2 earthquake are shown in Table 3, and the adjusted three kinds of seismic waves are shown in Figure 4.

Table 2: Supporting boundary condition.

Structural part		Support type
P0 pier	Upstream side	One-way movable support
	Downstream side	Two-way movable support
P1 pier	Upstream side	Consolidation
	Downstream side	Consolidation
P2 pier	Upstream side	Consolidation
	Downstream side	Consolidation
P3 pier	Upstream side	Consolidation
	Downstream side	Consolidation
P4 pier	Upstream side	One-way movable support
	Downstream side	Two-way movable support

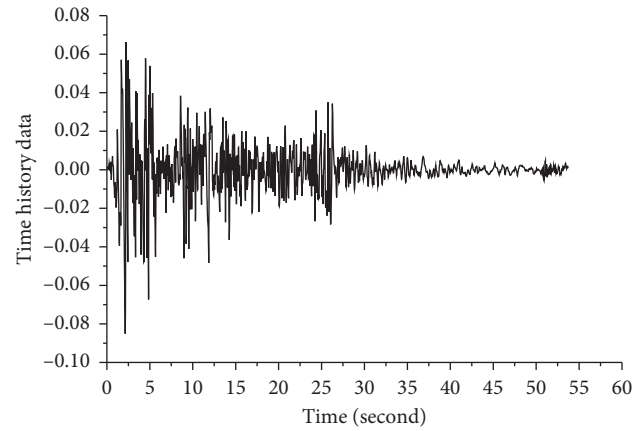

Figure 3: Time-history function of El Cento seismic wave after adjustment.

3.2. Realization of Traveling Wave Effects. In the process of seismic wave propagation, the time of seismic waves from the source to each station is different, and the effect caused by the time difference is called the traveling wave effect. The traveling wave effect must be considered in the seismic

Table 3: PGA adjustment coefficient of each seismic wave under the action of E2 earthquake.

Seismic wave	PGA adjustment factor
1979 James RD E1 Centro 220 Deg	0.2314
1994 Northridge Sylmar County Hosp 90 Deg	0.1406
Artificial wave	0.8149

analysis of the super large bridge. There are two main methods to analyze the seismic traveling wave effect of bridges by MIDAS, namely, inconsistent ground motion analysis method and mass method.

3.2.1. Nonuniform Ground Motion Analysis Method. With the propagation path of seismic wave, different seismic waves are set at different supports of the bridge, or the time difference of the same seismic wave arriving at each support of the bridge is set, to realize the simulation of different apparent wave velocities, which is called nonuniform ground motion analysis method. In this kind of ground motion analysis, the characteristics of seismic wave mode will not change, only the different apparent wave velocities and weakening amplitude will be changed. Supposing the acceleration function of n point on the ground is $\ddot{u}_n(t)$, the ground motion acceleration function of a point m on the seismic wave propagation path can be expressed as follows:

$$\ddot{u}_m(t) = C\ddot{u}_n\left(t - \frac{d}{v}\right). \tag{6}$$

Among them, C is the amplitude attenuation coefficient ($C \le 1$). When the attenuation along the length of the structure is not obvious, $C = 1$ represents the distance between the n point and m point on the seismic wave transmission path. v represents the velocity of seismic wave propagation.

3.2.2. Mass Method. When the bridge is subjected to an earthquake, the dynamic equation of each support is as follows:

$$\begin{bmatrix} M_s & 0 \\ 0 & M_b \end{bmatrix}\{\ddot{y}_s\ \ddot{y}_b\} + \begin{bmatrix} C_s & C_{sb} \\ C_{sb}^T & C_b \end{bmatrix}\begin{Bmatrix} \dot{y}_s \\ \dot{y}_b \end{Bmatrix} + \begin{bmatrix} K_s & K_{sb} \\ K_{sb}^T & K_b \end{bmatrix}\begin{Bmatrix} y_s \\ y_b \end{Bmatrix} = \begin{Bmatrix} 0 \\ F_b \end{Bmatrix}. \tag{7}$$

Here, M_s is the mass matrix at the support, M_b is the damping matrix at the support, $\ddot{y}_s$ is the acceleration of the ground motion at the nonsupport, $\ddot{y}_b$ is the seismic wave velocity at the nonsupport, C_s is the damping matrix at the nonsupport, C_b is the damping matrix at the support, $\dot{y}_s$ is the ground motion velocity at the nonsupport, $\dot{y}_b$ is the ground motion velocity at the support, K_s is the stiffness matrix of nonsupport, K_b is the damping matrix at the support, y_s is the displacement at the nonsupport, y_b is the displacement at the support, and F_b is the sum of forces from the ground.

The mass method assumes that a large mass element matrix M is attached to the support (usually more than 10^6 times of M_b). Under earthquake excitation, M and F_b can be expressed as follows:

$$M = \begin{bmatrix} M_1 & \cdots & 0 \\ 0 & \cdots & 0 \\ 0 & \cdots & M_n \end{bmatrix}. \tag{8}$$

In the formula, except that the diagonal element is M_i, the rest are 0.

$$F_b = M\ddot{y}_g, \tag{9}$$

where $\ddot{y}_g$ is the acceleration of the ground motion excited by the foundation.

The large mass matrix is brought into formula (8) and combined with formula (10)as follows:

$$\begin{bmatrix} M_s & 0 \\ 0 & M_b + M \end{bmatrix}\{\ddot{y}_s\ \ddot{y}_b\} + \begin{bmatrix} C_s & C_{sb} \\ C_{sb}^T & C_b \end{bmatrix}\begin{Bmatrix} \dot{y}_s \\ \dot{y}_b \end{Bmatrix} + \begin{bmatrix} K_s & K_{sb} \\ K_{sb}^T & K_b \end{bmatrix}\begin{Bmatrix} y_s \\ y_b \end{Bmatrix} = \begin{Bmatrix} 0 \\ M\ddot{y}_g \end{Bmatrix}. \tag{10}$$

We expand the second line in formula (11) to get the following results:

$$(M_b + M)\ddot{y}_b + C_{sb}^T\dot{y}_s + C_b\dot{y}_b + K_{sb}^T y_s + K_b y_b = M\ddot{y}_g. \tag{11}$$

Multiply both sides by M^{-1}, because the magnitude of M is quite large, therefore, $M^{-1} = 0$, formula (12) can be simplified as follows:

$$\ddot{y}_b \approx \ddot{y}_g. \tag{12}$$

4. Analysis of Seismic Response Parameters

Because of the structural characteristics of a single cable plane, steel truss, and semifloating system, the overall structure of a steel truss cable-stayed bridge with a single cable plane is relatively weak. Therefore, by changing the stiffness of the stayed cables, steel truss girder, and changing the structural system to analyze the seismic response parameters of the bridge, the transformation of the three parameters does not change the bridge type and can be realized from the finite element software and the actual project. By changing the elastic modulus of stay cables and steel truss members, the change of stiffness is simulated without changing any section characteristic parameters. By changing the connection constraints between the tower and girder and the type of support at the pier, the transformation of several systems is realized. The bending moment direction of the bridge tower is My, and the displacement of the bridge tower and the displacement of the lower chord of the steel truss girder refer to the spatial displacement. The

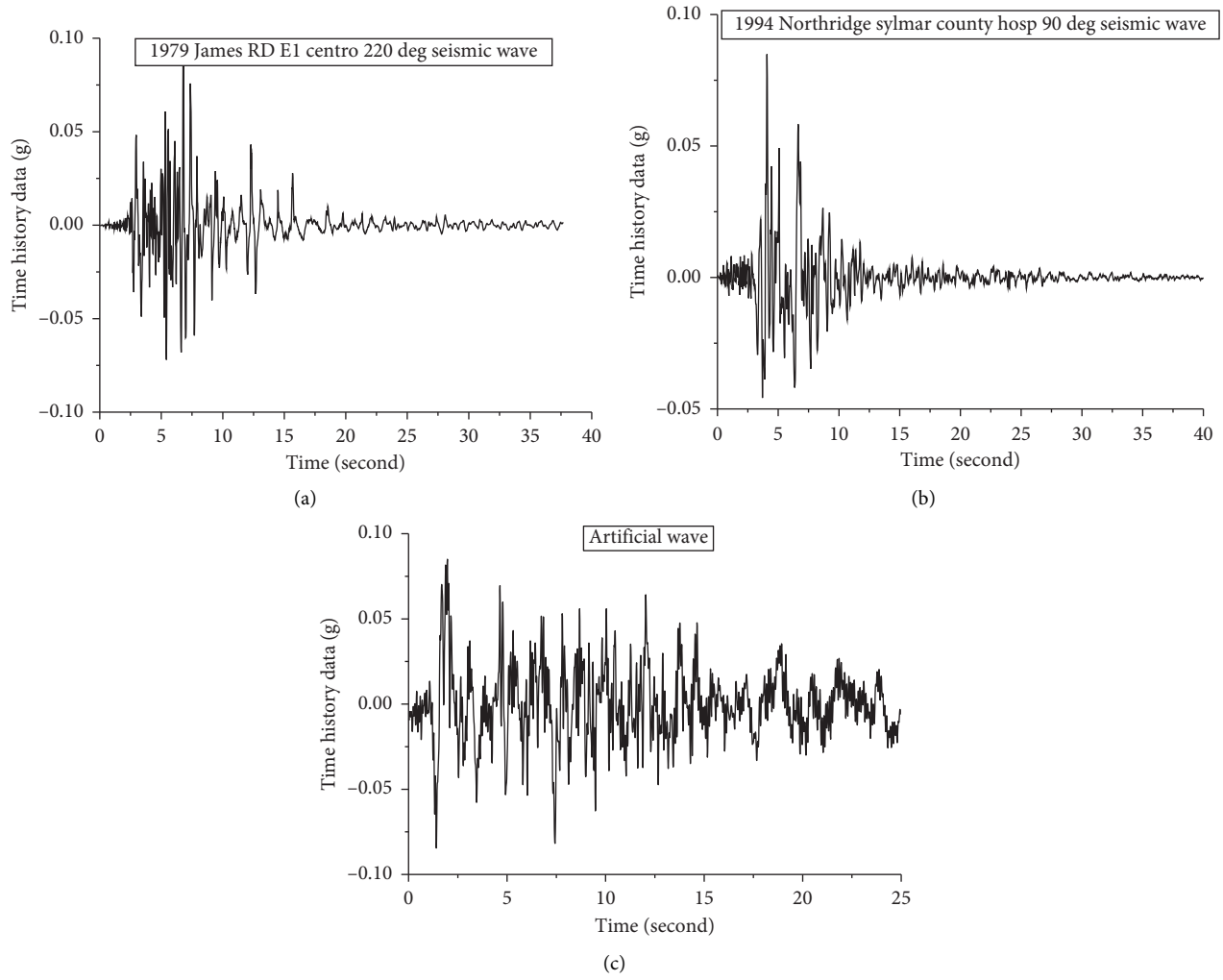

Figure 4: Time-history functions of three kinds of seismic waves after adjustment. (a) 1979 James RD E1 Centro 220 Deg, (b) 1994 Northridge Sylmar County Hosp 90 Deg, and (c) artificial wave.

displacement and axial force of steel truss members are taken from the outermost bottom chord on the right side.

4.1. Influence of Cable Stiffness Variation on Seismic Response of the Bridge. The changes in the stiffness of the stayed cable are simulated by changing the multiple changes of the elastic modulus of the material used in the stay cable. Since the material and section of the actual structure are more reasonable when the stiffness of the stay cable is 0.6 times to 1.6 times, it is not possible to exceed this range. The multiple changes were 0.6, 0.8, 1.2, 1.4, and 1.6 times, respectively. When analyzing the influence of stay cable stiffness change on the bending moment and displacement of the tower and the axial force and displacement of the lower chord of steel truss girder under seismic action along bridge-transverse bridge coupling direction, all the data are taken as the maximum value under the earthquake action. The distribution of the maximum displacement U and bending moment My along the tower height of the bridge with different multiple cable stiffness under earthquake action is shown in Figures 5(a) and 5(b). The longitudinal distribution of the maximum displacement, U, and axial force, Fx, of the outermost bottom chord on the right side of the steel truss girder along the bridge deck with different multiple cable stiffness under earthquake action is shown in Figure 6.

The influence of the change of cable stiffness on the displacement of bridge towers under earthquake action is mainly concentrated when the tower height is higher than 100 m. Because when the height of the tower is more than 100 m, the width of the tower will gradually narrow. It will be more sensitive to seismic action, and the upper 141 m to 172 m is the cable area, and the change of cable stiffness will cause the change of cable area stiffness. When the height of the tower is higher than 100 m, the greater the stiffness of the stay cable, the smaller the displacement of the tower under earthquake action. Because the stiffness of the stay cable increases, the stiffness of the connection part between the tower and the stay cable is greater, to reduce the displacement of the tower under earthquake action when the height of the tower is higher than 100 m. When the tower height is 182 m, the displacement U of the bridge tower with 0.6 times

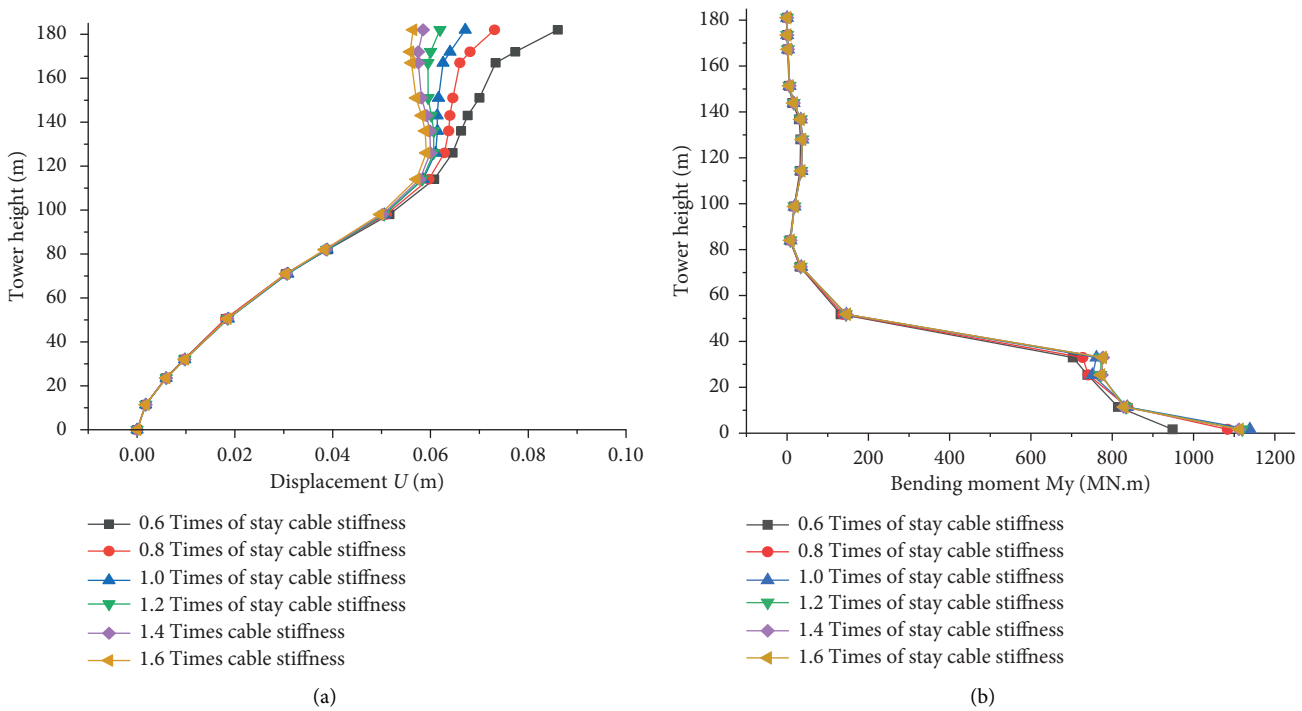

Figure 5: Distribution of maximum displacement U and maximum bending moment My along with the tower height for bridges with different multiples of cable stiffness under earthquake action. (a) Distribution of the maximum values of the tower displacement and (b) distribution of the maximum values of the tower bending moment.

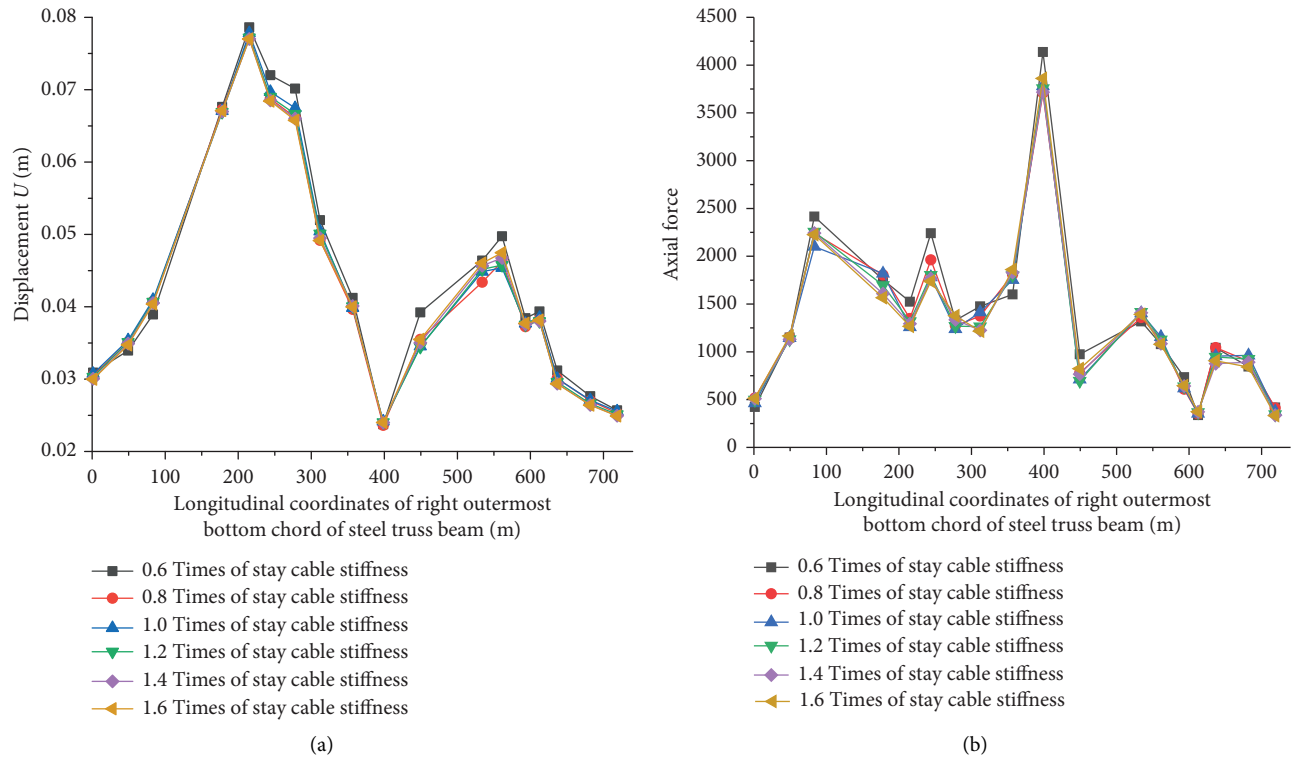

Figure 6: Longitudinal distribution of maximum displacement U and maximum axial force Fx of the bottom chord of the bridge with different multiple cable stiffness under earthquake action. (a) Longitudinal distribution of the maximum values of the displacement and (b) longitudinal distribution of the maximum value of the axial force.

the cable stiffness is the largest, which is 0.0861 m. However, the displacement U of the bridge tower with 1.6 times the cable stiffness is the smallest, which is 0.0565 m, with a decrease of 34.4%. It can be seen that the increase in cable stiffness can reduce the displacement of the tower under an earthquake. Selecting steel with appropriate stiffness as the stayed cable and increasing the stiffness as much as possible under the condition of ensuring flexible performance can reduce the effect of the earthquake on the displacement of the bridge tower.

The change of the stiffness of the stay cable has an obvious influence on the bending moment of the bridge tower under earthquake action only when the height of the bridge tower is less than 40 m, and the bending moment My of the bridge tower under earthquake action has no definite relationship with the stiffness of stay cable because the seismic force of bridge tower is mainly transmitted from the pier and main girder, even if the increase of the stiffness of stay cable has little influence on the seismic force of bridge tower. When the tower height is 0 m and the cable stiffness is 0.6 times, the bending moment of the bridge tower under earthquake action is the minimum, and when the cable stiffness is 1.0 times, the bending moment of the bridge tower under earthquake action is the maximum. When the tower height is 37 m, the bending moment of the bridge tower under earthquake action is the smallest when the cable stiffness is 0.6 times, and the bending moment of the bridge tower under earthquake action is very close when the cable stiffness is 1.0, 1.2, 1.4, and 1.6 times. In the case of using different diagonal cable stiffness, the bending moment at the base of the bridge tower is more influenced by it.

When the longitudinal coordinate of the deck is 400 m, the displacement of the bottom chord of the steel truss girder is the smallest under the earthquake action, because this is the junction of the tower and the girder, and usually the seismic response displacement of the junction of the tower and the girder of the cable-stayed bridge is the smallest. The change of cable stiffness has little influence on the displacement of the steel truss girder under earthquake action, and the six curves shown in Figure 5(a) are more concentrated. Although the increase of stay cable stiffness will increase the stiffness of the connection part between the steel truss girder and the stay cable, because the layout of the stay cable of this bridge is a thin cable with a single cable plane, and the connection part between stay cable and steel truss girder is too local compared with the total length of 720 m, so as long as the stay cable stiffness is not small, the influence of the change of stay cable stiffness on the displacement of steel truss girder under earthquake action is very small.

The change of cable stiffness has little effect on the axial force FX of the lower chord of the steel truss girder under earthquake action. With the change of cable stiffness, the variation range of axial force of the lower chord of steel truss girder under earthquake action is not large. Even when the longitudinal coordinate is 400 m (at the junction of the bridge tower and steel truss girder), the axial force under earthquake action is only slightly different when the cable stiffness is 0.6 times.

4.2. Influence of Stiffness Variation of Steel Truss Girder on Seismic Response of the Bridge. The change of steel truss stiffness is simulated by changing the multiple elastic moduli of steel truss material, and the multiple transformations are 0.6, 0.8, 1.2, 1.4, and 1.6 times, respectively. When analyzing the influence of stiffness parameters of steel truss girder on the bending moment and displacement of the bridge tower and the axial force and displacement of the lower chord of steel truss girder under the seismic action along the bridge-transverse bridge coupling direction, all the data are taken from the maximum value under the earthquake action. The distribution of the maximum displacement U and bending moment My along the tower height of the bridge with different multiple steel truss stiffness under earthquake action is shown in Figure 7, and the distribution of the maximum displacement U and axial force Fx along the longitudinal direction of the bridge deck of the bridge with different multiple steel truss stiffness under earthquake action is shown in Figure 8.

The change of steel truss girder stiffness has an obvious influence on the displacement U of the bridge tower under earthquake action. When the tower height is less than 120 m, the influence is greater when the tower height is more than 120 m, and the influence is the biggest when the tower height is 182 m. With the increase of steel truss girder stiffness, the displacement of the bridge tower under earthquake action decreases, because the displacement of the bridge tower under earthquake action in the cable area (141 m to 172 m) is affected by the middle and lower parts of the bridge tower and cable-stayed bridge. When the stiffness of the steel truss girder increases, the earthquake action transmitted by the stay cables decreases, and the stiffness of the connection between the tower and the steel truss girder increases. When the tower height is 182 m, the maximum displacement of the bridge tower under earthquake action is 0.085 m when the steel truss stiffness is 0.6 times, and the minimum displacement of the bridge tower under earthquake action is 0.067 m when the steel truss stiffness is 1.6 times, with a decrease of about 21.8%. It can be seen that the increase in the stiffness of the steel truss girder can reduce the displacement of the bridge tower under earthquake action.

The influence of the stiffness of the steel truss girder on the bending moment My of the bridge tower under earthquake action is obvious below 40 m. At the root of the bridge tower (when the height of the bridge tower is 0 m), the bending moment of the bridge tower with 0.8 times the steel truss girder stiffness is the largest under earthquake action. However, when the height of the tower is 37 m, the bending moment of the tower with 0.8 times the steel truss girder stiffness is the smallest under earthquake action. Under different tower heights, the influence of steel truss girder stiffness on the bending moment of bridge towers under earthquake action is not consistent. It can be seen that the mechanism of the influence of the stiffness change of steel truss girder on the bending moment of bridge tower is pretty complex and needs further study.

The influence of the change of steel truss girder stiffness parameters on the displacement of steel truss bottom chord under earthquake action is mainly concentrated in the range

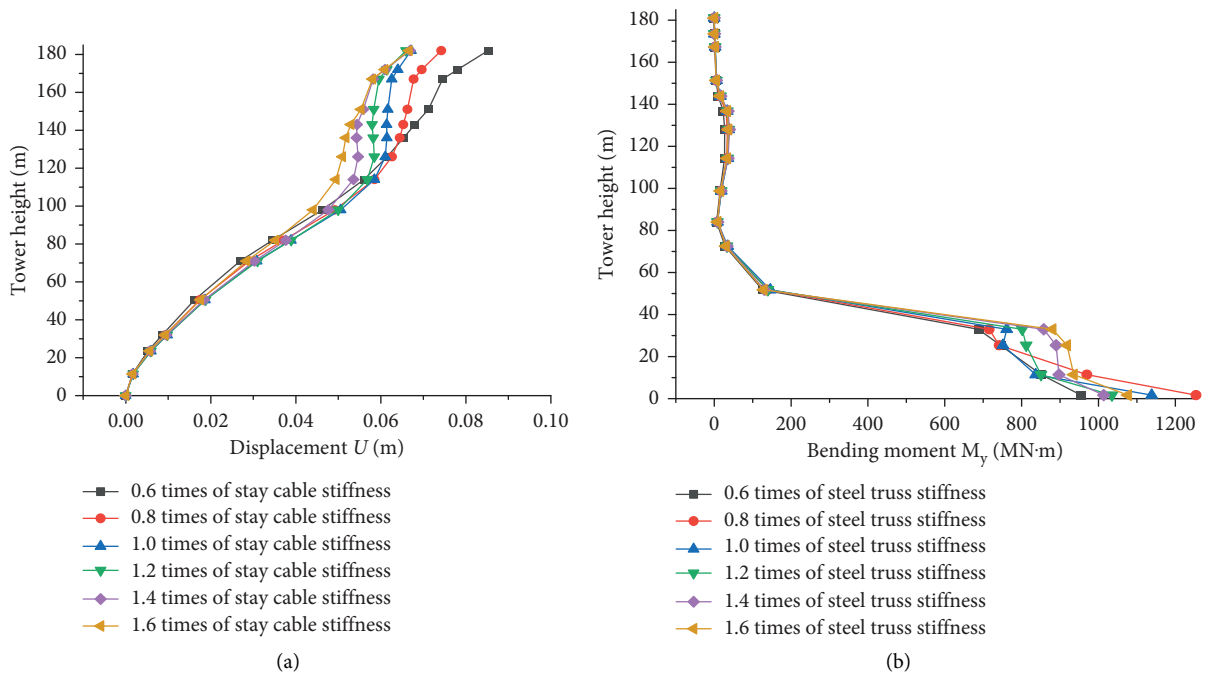

Figure 7: Distribution of maximum displacement U and maximum bending moment My along with the tower height for bridges with different multiples of steel joist stiffness under earthquake action. (a) Distribution of the maximum value of the bridge tower displacement and (b) distribution of the maximum value of the bridge tower bending moment.

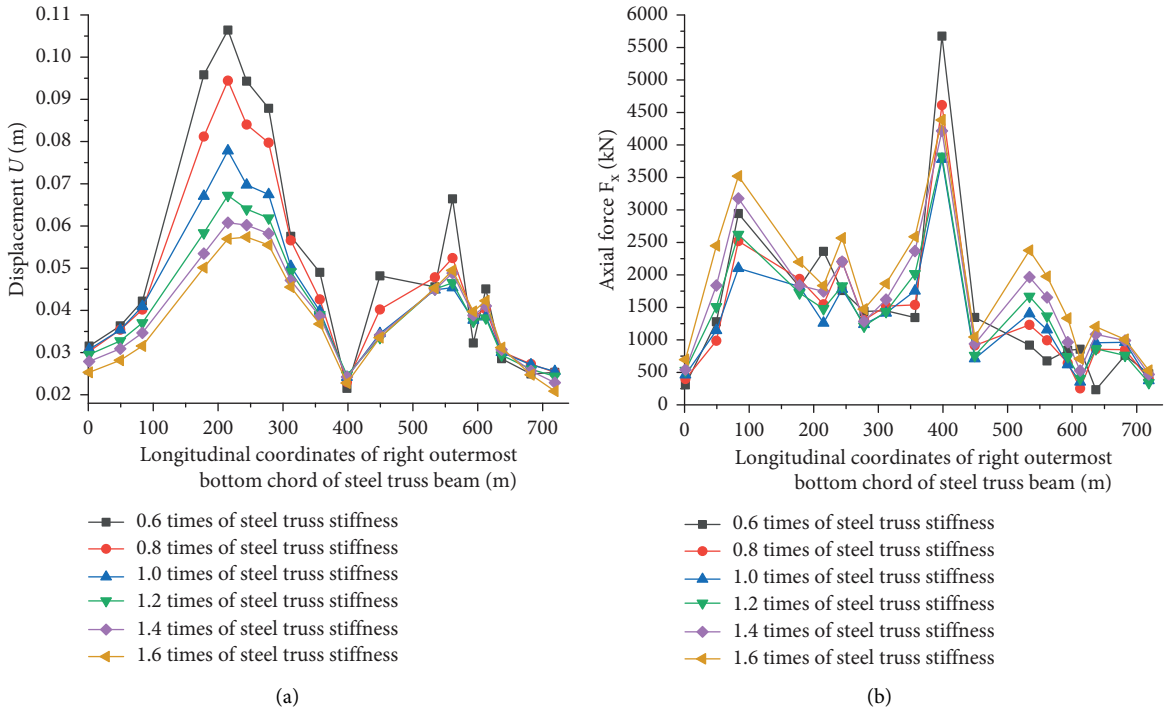

Figure 8: Longitudinal distribution of chord displacement U and axial force Fx along with the bridge deck for bridges with different multiples of steel joist stiffness under earthquake action. (a) Longitudinal distribution of the maximum value of the displacement and (b) longitudinal distribution of the maximum value of the axial force.

of 88 m–400 m, which is the whole span of the main span of a cable-stayed bridge. The main span is larger, and the displacement under earthquake action is more sensitive. With the increase of the multiple steel truss girder, the displacement of the bottom chord of the steel truss girder under earthquake action decreases, because the steel truss girder is

the most important component of the bridge. When the stiffness of the steel truss girder increases, the stiffness of the connection between the steel truss girder and bridge tower increases, and the displacement decreases. At the same time, the displacement transmitted by stay cables under seismic action also decreases. When the longitudinal coordinate is 244 m (in the middle of the main span), the influence is most obvious. When the stiffness of the steel truss girder is 0.6 times, the displacement of the bottom chord of the steel truss girder is the largest, which is 0.048 m. When the stiffness of the steel truss girder is 1.6 times, the displacement of the bottom chord of the steel truss girder is the smallest, which is 0.034 m, with a decrease of 30.4%. It can be seen that increasing the stiffness of steel truss girder can reduce the displacement of steel truss girder under earthquake action.

The change of steel truss girder stiffness has a great influence on the axial force of the bottom chord of the steel truss girder under earthquake action, and the axial force curve fluctuates in the whole range of longitudinal coordinates because the steel truss members are connected to transfer internal force. When the longitudinal coordinate is 88 m (at the side pier of the main span), the axial force of the bottom chord of the steel truss girder is the smallest when the stiffness of the steel truss girder is 1.0 times, and the axial force of the bottom chord of the steel truss girder is the largest when the stiffness of the steel truss girder is 1.6 times. When the longitudinal coordinate is 400 m (at the junction of tower and girder), the axial force of the bottom chord of the steel truss girder is the smallest when the stiffness of the steel truss girder is 1.0 times, and the axial force of the steel truss girder is the largest when the stiffness of the steel truss girder is 0.6 times, with the variation amplitude of 33.4%. Under different longitudinal coordinates, the influence of the change of the stiffness of the steel truss girder on the axial force of the bottom chord of the steel truss girder under earthquake action is not consistent, and there is no uniform law. Because the steel truss girder is different from the steel box girder, the steel truss girder is composed of a variety of members, the distribution of the top chord, and web member, and bottom chord is different, and there is the transfer of bending moment, axial force, displacement, etc., between all kinds of members. The bottom chord is not simply connected to the adjacent bottom chord, so it is difficult to have a uniform law.

4.3. Influence of Structural System Changes on Seismic Response of the Bridge. The semifloating system of the original structure is changed into a floating system, rigid frame system, and tower girder consolidation system. The transformation of several systems can be realized by changing the connection constraints of the tower girder and the supports at piers. The structural diagrams of several systems are shown in Figure 9. When analyzing the influence of structural system parameter changes on the bending moment My and displacement U of the tower and the axial force Fx and displacement U of the bottom chord of steel truss girder under earthquake action along bridge-transverse bridge coupling direction, all data are taken from the maximum value under the action of ground motion. The distribution of the maximum displacement U and bending moment My along the tower height of bridges with different structural systems under earthquake action is shown in Figure 10. The distribution of the maximum displacement U and axial force Fx along the longitudinal direction of the bridge deck of bridges with different structural systems under earthquake action is shown in Figure 11.

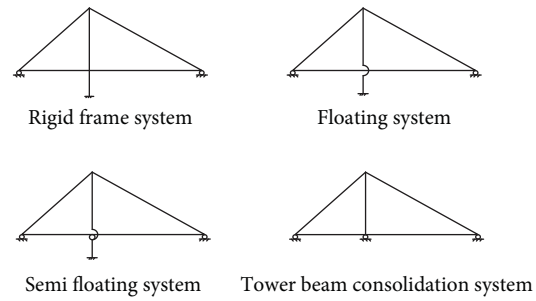

Figure 9: Several systems of a cable-stayed bridge with a single tower.

When the height of the bridge tower is less than 130 m, the displacement of the floating system under seismic action is the smallest, but when the height of the bridge tower is more than 130 m, the displacement of the floating system under seismic action is the largest, because the floating system is characterized by the freedom between the tower and the girder. When the height of the bridge tower is less than 130 m, the bridge tower only accepts the seismic action transmitted by the pier and is slightly affected by the indirect seismic action transmitted by the main girder through the stay cables. When the tower height is higher than 130 m, the seismic action of the bridge tower is more affected by the stay cables, and the tower girder is only indirectly connected by the stay cables, which increases the transmission of earthquake action between the tower and the girder. In addition to the floating system, the displacement of the other three systems under earthquake action is relatively close, especially the displacement curves of the semifloating system and the tower girder consolidation system under earthquake action almost coincide, and the displacement of the rigid frame system under earthquake action is the smallest, because the tower girder consolidation system is very similar to the semifloating system, and the rigid frame system makes the stiffness of the whole bridge larger.

The bending moment of the floating system is the smallest under the earthquake action, and the bending moment of the other three systems is very close under the earthquake action, and the distribution law is consistent. In addition to the floating system, there are connections between the floating system and the tower girder of the three systems, and the connection between the tower girders will transfer the bending moment, which makes the bending moment of the bridge tower under earthquake action amplified.

With the enhancement of the longitudinal restraint between the tower and the beam, the maximum value of the displacement at the top of the tower is significantly reduced,

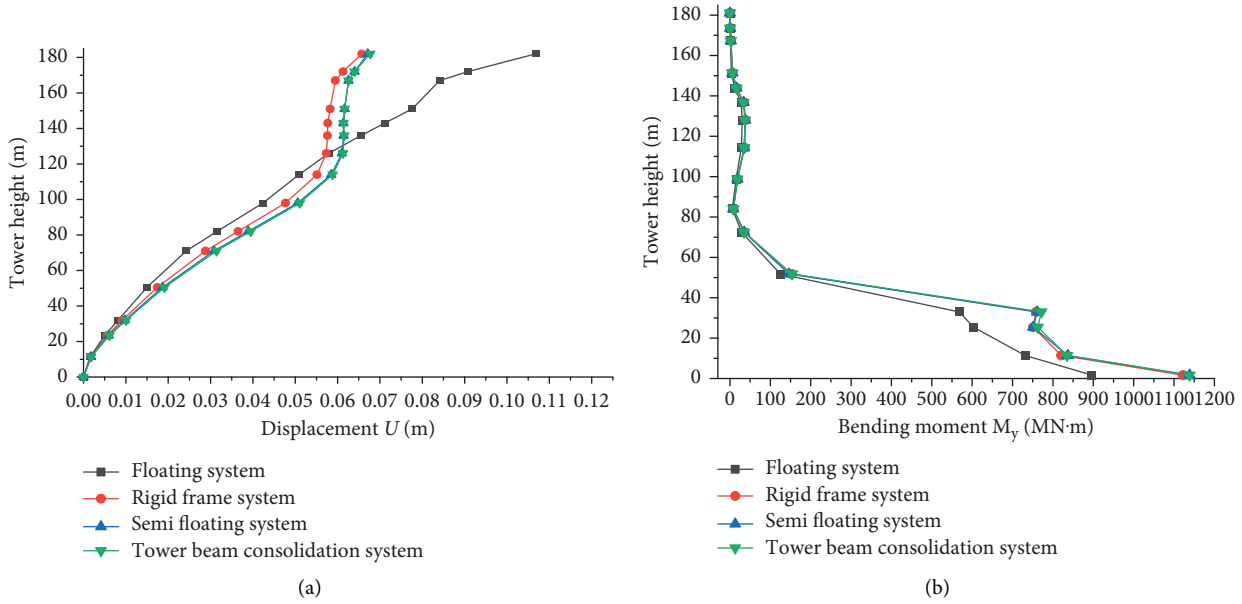

Figure 10: Distribution of maximum displacement U and maximum bending moment My along with the tower height for bridges of different structural systems under earthquake action. (a) Distribution of the maximum value of the bridge tower displacement and (b) distribution of the maximum value of the tower bending moment.

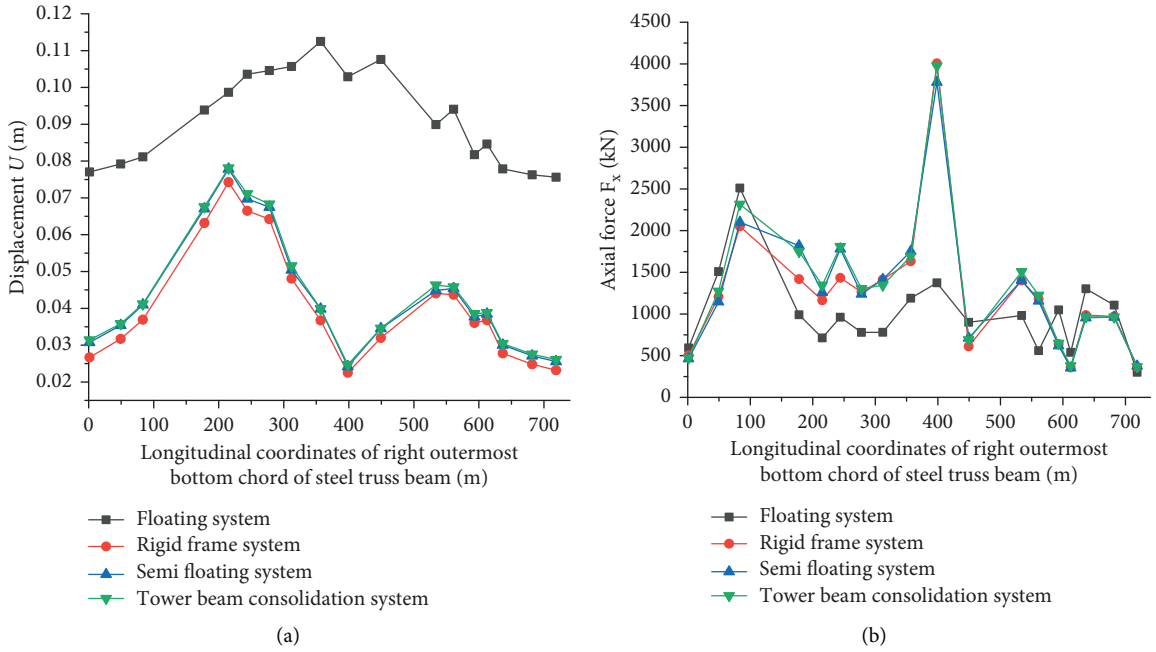

Figure 11: Longitudinal distribution of maximum chord displacement U and maximum axial force Fx of bridges with different structural systems under earthquake action. (a) Longitudinal distribution of the maximum value of the displacement and (b) longitudinal distribution of the maximum value of the axial force.

and the maximum value of the bending moment at the bottom of the tower is significantly increased. From the magnitude of the effect of traveling waves on the displacement and bending moment of the model, the longitudinal restraint between the tower and the beam and the type of restraint play a nonnegligible role.

The law of the bottom chord of the floating steel truss system under earthquake action is different from that of the other three systems, as shown in Figure 11. The displacement of the bottom chord of the steel truss girder of the floating system is very large under earthquake action. The displacement of the bottom chord of the steel truss girder of the other three systems under earthquake action is close. The displacement of the rigid frame system under earthquake action is the smallest because the connection between the tower and the girder can reduce the displacement under

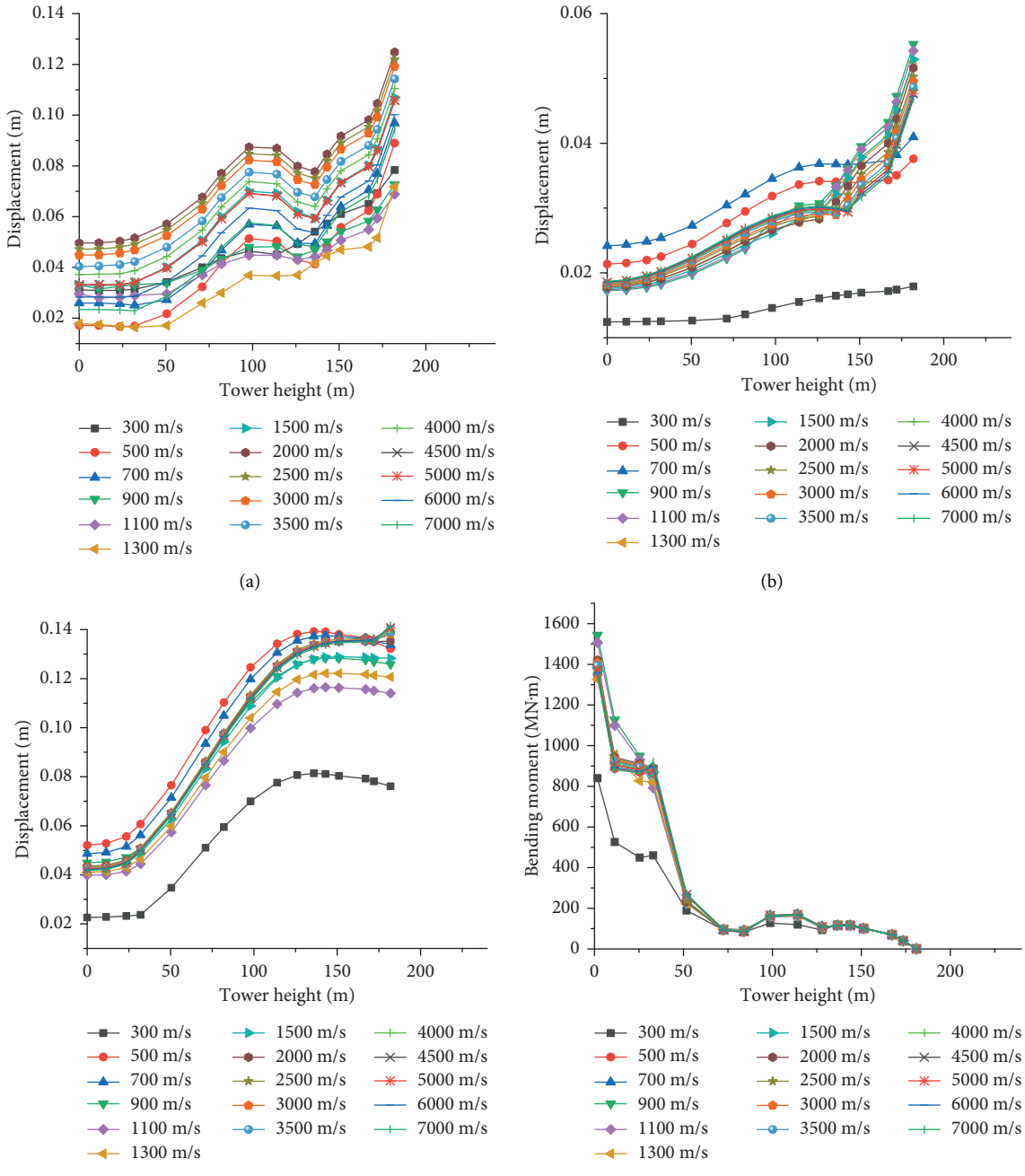

Figure 12: Continued.

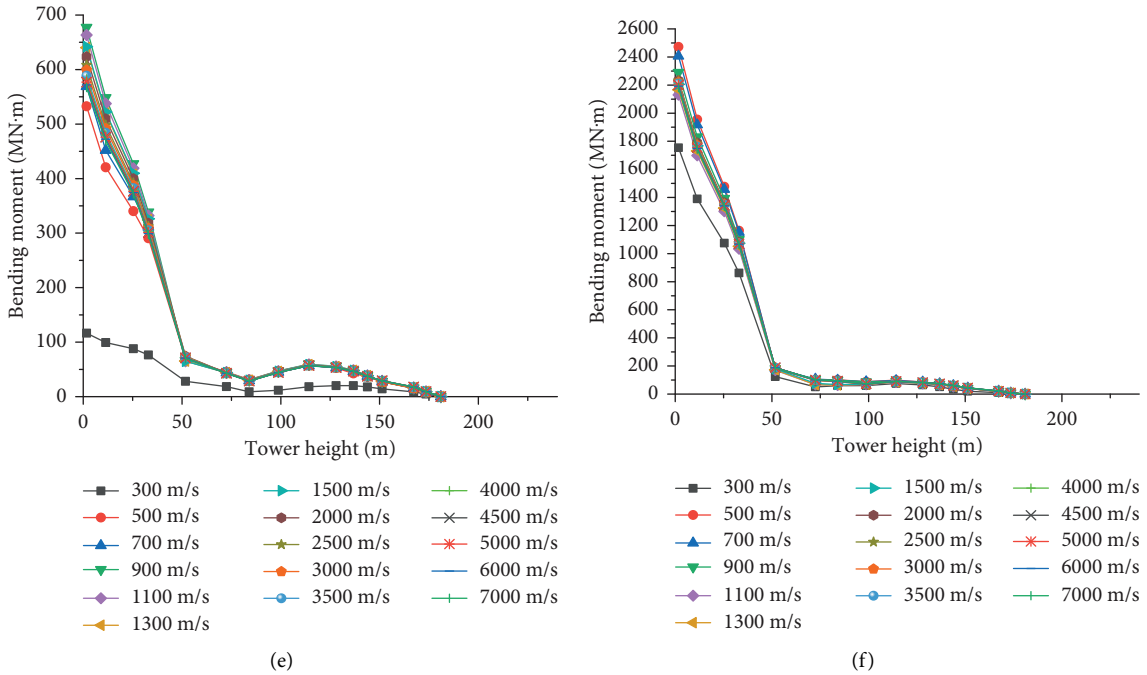

Figure 12: Distribution of maximum displacement and maximum bending moment along with the tower height under three kinds of seismic waves with different apparent wave velocities. (a) 1979 James RD E1 Centro 220 Deg seismic wave, (b) 1994 Northridge Sylmar County Hosp 90 Deg seismic wave, (c) the artificial wave, (d) 1979 James RD E1 Centro 220 Deg seismic wave, (e) 1994 Northridge Sylmar County Hosp 90 Deg seismic wave, and (f) the artificial wave.

earthquake action. However, there is no connection between the steel truss girder of the floating system and the bridge tower, and the steel truss loses the vertical stability of the bridge tower. The lateral support makes the displacement of the steel truss girder large. The overall stiffness of the rigid frame system is quite large, and the displacement of the steel truss girder is the smallest.

The axial force distribution of the bottom chord of the steel truss girder of the floating system under earthquake action is different from that of the other three systems. When the longitudinal coordinate of the other three systems is 400 m, the axial force under earthquake action has an extreme value, but the floating system does not, because there is no connection between the tower and the main girder of the floating system, and 400 m is just the tower girder connection. The axial force of the bottom chord of the floating system is smaller than that of the other three systems under earthquake action, while the distribution of the other three systems is the same and the fluctuation is very small.

5. Seismic Analysis of Traveling Wave Effect

Three kinds of seismic waves with different PGA, spectrum characteristics, and ground motion duration are selected. At present, the apparent wave velocity of recorded seismic waves is mainly between 300 m/s and 7000 m/s. Therefore, the apparent wave velocity of each kind of seismic wave is set in this range. This chapter explores the influence of the traveling wave effect on the cable tower and steel truss girder of steel truss cable-stayed bridge with a single tower and a single cable plane. In Figures 12 and 13, the responses of the 1979 James RD E1 Centro 220 Deg seismic wave, 1994 Northridge Sylmar County Hosp 90 Deg seismic wave, and an artificial wave are shown from left to right, respectively.

5.1. Seismic Response Analysis of Cable Tower. Under the action of the earthquake, the cable tower will deform, and each section will produce internal force. Under the action of three kinds of seismic waves, the apparent wave velocity of each kind of seismic wave is set between 300 m/s and 7000 m/s, and the distribution of the maximum displacement and bending moment of the cable tower along the tower height is shown in Figure 12 (the coordinate of tower base is 0 m, the coordinate of upper tower top is 182 m, and the tower height is 182 m in total).

Although the three seismic waves selected in this paper reach a consistent peak acceleration of 0.085 g after amplitude modulation, the differences in spectral characteristics and duration lead to different manifestations of the traveling wave effect of the structure under the influence of each seismic wave. On the left side is the response diagram of the 1979 James RD E1 Centro 220 Deg seismic wave. The variation law of maximum displacement with tower height is consistent under each apparent wave velocity, first increases then decreases, and finally increases. When the apparent wave speed is 900–1300 m/s and 2000–4000 m/s, the maximum displacement of the tower will increase significantly with the decrease of the apparent wave speed. When the apparent wave speed is 2000 m/s, the displacement of the

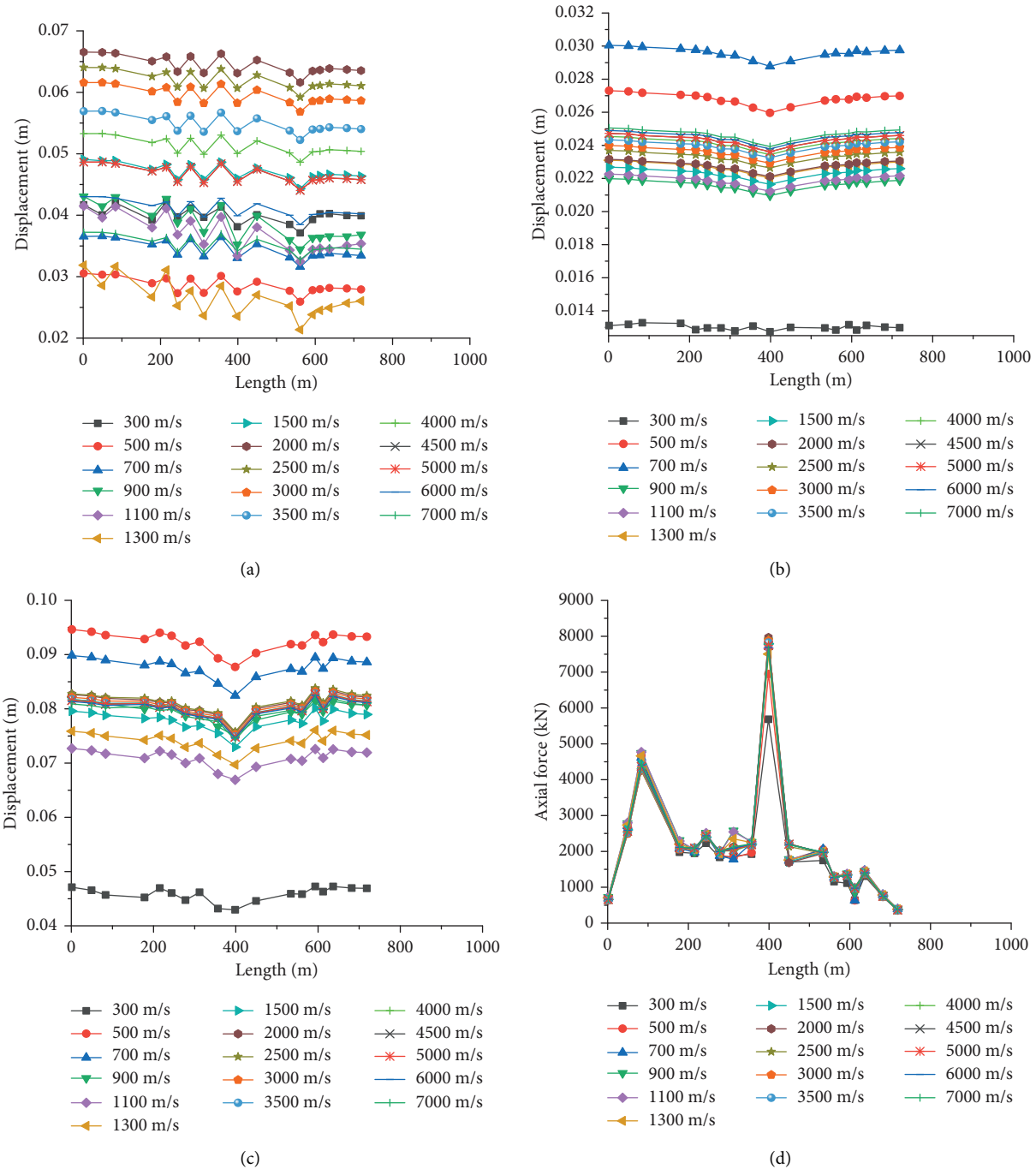

Figure 13: Continued.

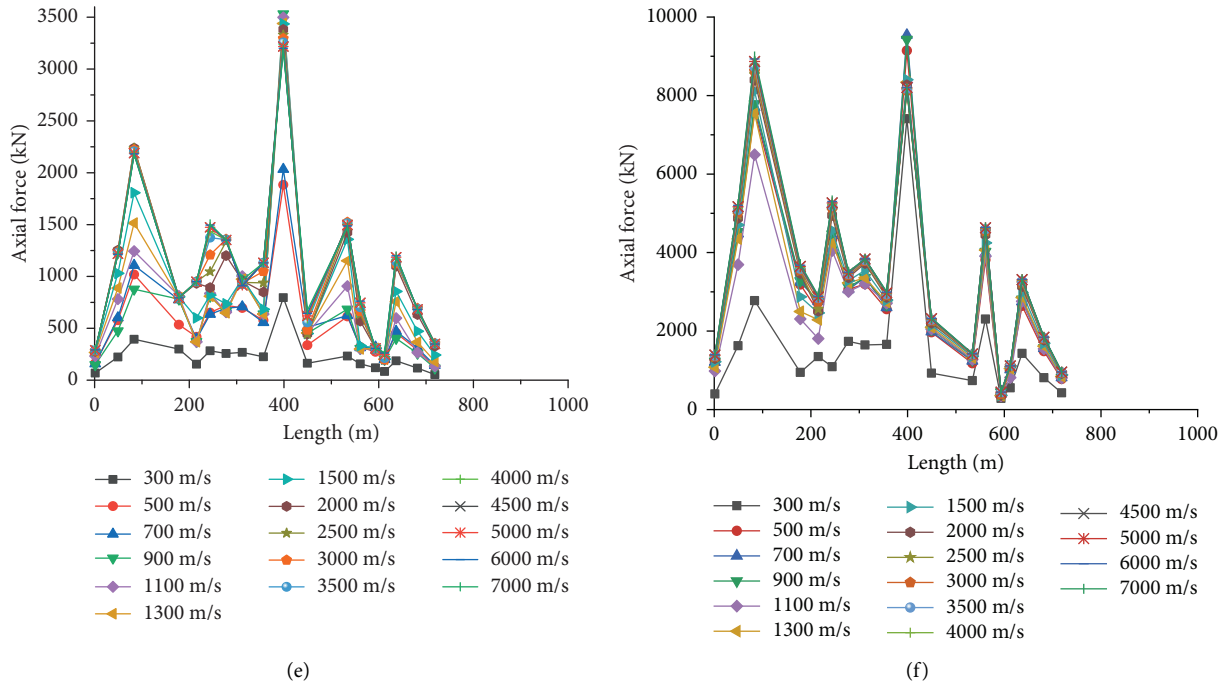

Figure 13: Distribution of maximum displacement and maximum axial force with the length of steel truss main girder under three kinds of seismic waves with different apparent wave velocities. (a) 1979 James RD E1 Centro 220 Deg seismic wave, (b) 1994 Northridge Sylmar County Hosp 90 Deg seismic wave, (c) artificial wave, (d) 1979 James RD E1 Centro 220 Deg seismic wave, (e) 1994 Northridge Sylmar County Hosp 90 Deg seismic wave, and (f) artificial wave.

tower top is the maximum value. In the middle is the response diagram of the 1994 Northridge Sylmar County Hosp 90 Deg seismic wave, and the maximum displacement increases slightly at first and then sharply with the tower height at each apparent wave velocity. When the apparent wave speed is 300–700 m/s, the maximum displacement of the tower increases significantly with the increase of the apparent wave speed. When the apparent wave speed is 900 m/s, the displacement of the top of the tower is the maximum value. On the right side is the response diagram under the action of the artificial wave, and the maximum displacement at each apparent wave speed increases first and then tends to be constant with the tower height. Although the peak acceleration of the three selected seismic waves has been adjusted to 0.085 g, due to their different spectral characteristics, the variation law of the maximum displacement of the cable tower along with the tower height under different apparent wave velocities of the three seismic waves is not completely consistent.

The distribution of the maximum bending moment of the cable tower with the tower height is similar under the three kinds of seismic waves with different apparent wave velocities, which all drop sharply at first, then slowly, and finally become very small. However, the maximum bending moment values corresponding to the height of the cable tower under the action of the earthquake are different, and the bending moment values corresponding to each tower height under the action of artificial waves are relatively large. The results show that the variation of the maximum bending moment of the cable tower is still similar under the action of seismic waves with different spectrum characteristics and duration of ground motion. The variation of the maximum bending moment of the cable tower under the action of the earthquake is less affected by the different spectrum characteristics and duration of ground motion, but the maximum bending moment under the action of the earthquake is still affected, and the effective time of artificial wave is pretty long and does not change during the effective time. The bending moment of the tower is the largest under the action of the artificial wave.

Under the action of three kinds of seismic waves, when the apparent wave velocity is greater than 300 m/s, with the increase of the apparent wave velocity, the distribution curve of the maximum bending moment of the cable tower with the tower height under each apparent wave velocity is more concentrated, which indicates that the maximum bending moment of the cable tower under earthquake action is not a sensitive factor in the study of traveling wave effect. When the apparent wave velocity is small, the time difference of seismic waves arriving at each pier of the bridge is large, and even the nonsensitive factors will be unstable at low wave velocity, which is worthy of attention.

5.2. Seismic Response Analysis of the Main Girder. Under the action of the earthquake, the main girder of the steel truss will deform, and the internal force of each section will also be produced. Under the action of three kinds of seismic waves, the apparent wave velocity of each kind of seismic wave is set between 300 m/s and 7000 m/s. With the change of bridge length, a certain member of each length is selected for research. The distribution of maximum displacement and

maximum axial force of members with bridge length is shown in Figure 13.

Similar to the effect of the traveling wave effect on the maximum displacement of the cable tower, the maximum displacement of the steel joist main beam bar fluctuates more with the change of apparent wave velocity when it is in the lower apparent wave velocity range under the 1994 Northridge Sylmar County Hosp 90 Deg seismic and artificial wave effects. After the apparent wave velocity reaches a certain value, the maximum displacement of the steel joist main beam bar fluctuates more with the increase of apparent wave velocity at each apparent wave velocity. The maximum displacements of steel joist main beam with length are more concentrated after the apparent wave velocity reaches a certain value, but there is no such pattern under the 1979 James RD E1 Centro 220 Deg seismic wave. Under the effect of the 1979 James RD E1 Centro 220 Deg seismic wave, when the apparent wave velocity is 900–1300 m/s and 2000–4000 m/s, the maximum displacement of steel joist main beam increases with the decrease of apparent wave velocity, just like the variation of maximum displacement of cable tower.

The results show that the distribution of the maximum axial force with the length of the main girder of the steel truss under different apparent wave velocities of the three kinds of seismic waves is generally similar, which first increases to 88 m and then decreases with the length of the bridge and fluctuates between 88 m and 360 m, increases sharply from 360 m to 400 m, decreases sharply from 400 m to 440 m, and fluctuates between 440 m and 720 m. However, the values of the maximum axial force corresponding to the length of the bridge are different, which indicates that the variation of the maximum axial force of the main girder is less affected by the spectrum characteristics and the duration of the ground motion. However, the maximum axial force of earthquake action is still greatly affected.

Under the action of three kinds of seismic waves, when the apparent wave velocity is greater than a certain value, with the increase of the apparent wave velocity, the distribution curve of the maximum axial force value of the steel truss main girder member with the bridge length under each apparent wave velocity is more concentrated, which indicates that when the apparent wave velocity is greater than a certain value, the maximum axial force value of the steel truss main girder member is less affected by the apparent wave velocity, but the critical apparent wave velocity value of each seismic wave is different.

6. Conclusion

The parameters analysis of the seismic response of steel truss cable-stayed bridges with a single tower and a single cable plane is of universal significance, which can provide a reference for similar bridges. In this paper, the nonlinear time-history analysis method and nonuniform seismic analysis method are used to investigate the influence of structural parameters and traveling wave effect on the seismic response of steel truss cable-stayed bridge with a single tower and a single cable plane.

(1) When the tower reaches a certain height, the greater the cable stiffness, the smaller the displacement of the tower under seismic action, i.e., the increase of cable stiffness can optimize the displacement of the tower under seismic action; the change of cable stiffness has little effect on the tower bending moment, steel truss beam displacement, and axial force under seismic action.

(2) The increase of steel joist stiffness can reduce the displacement of the bridge tower and steel joist under earthquake. The increase of steel joist stiffness can optimize the displacement of the bridge tower and steel joist under earthquake.

(3) The specific seismic response analysis shows that the change in the stiffness of the diagonal cable and steel truss beam has a significant effect on the bottom bending moment of the tower, and the main influence range is concentrated in the tower height of 0~40 m.

(4) In general, the displacement under seismic action of the floating system is larger than the other three systems, but the internal force under seismic action is significantly smaller than the other three systems. The presence or absence of longitudinal restraint and the form of restraint play a nonnegligible role in terms of the magnitude of the effect of traveling waves on the internal forces and displacements of the structure.

(5) The distribution pattern of the maximum bending moment with tower height and the distribution pattern of maximum axial force along the length of the bridge for the main girder rod under seismic action are less affected by the spectral characteristics and the duration of ground shaking, but the spectral characteristics and the duration of ground shaking have more influence on the values of maximum bending moment corresponding to the height of the tower and the values of maximum axial force for the main girder rod corresponding to the length of the bridge under seismic action.

(6) Under the 1979 James RD E1 Centro 220 Deg seismic wave, the maximum displacement of the cable tower and the maximum displacement of the main beam of the steel truss increase significantly with the decrease of the apparent wave speed when the apparent wave speed is between 900~1300 m/s and 2000~4000 m/s.

(7) When the apparent wave speed is small, the time difference of seismic waves reaching each pier of the bridge is large, and even nonsensitive factors will behave unstably at low wave speed, which deserves attention. The steel truss cable-stayed bridges with a single tower and a single cable plane are more prone to damage when seismic waves with the same peak acceleration, longer effective duration, and less attenuation act on the bridge.

(8) The variation of some parameters has obvious characteristics and patterns, but the mechanism of

the effect on specific structural internal forces is not clear. There is no universality of the effect of the change of steel joist stiffness parameter on the internal force of the bridge structure and the effect of traveling wave on the displacement of the bridge structure in a specific apparent wave speed interval.

Data Availability

All data included in this study are available upon request by contact with the corresponding author.

Conflicts of Interest

The authors declare that they have no conflicts of interest.

Acknowledgments

The authors appreciate the financial support from the Natural Science Foundation of China (Grant no. 51908093), State Key Laboratory of Mountain Bridge, Tunnel Engineering Development Fund (CQSLBF−Y14 and CQSLBF−Y16−10), and Chongqing Returned Overseas Students' Entrepreneurship and Innovation Support Fund (cx2018113 and cx202011).

References

[1] JTGTB02-01-2008, *Detailed Rules for Seismic Design of Highway Bridges*, People's Communications Press, 2020.

[2] C. Li, H. Li, H. Zhang, J. Su, R. Li, and Y. Ding, "Seismic performance evaluation of large-span offshore cable-stayed bridges under non-uniform earthquake excitations including strain rate effect," *Science China Technological Sciences*, vol. 63, no. 7, pp. 1177–1187, 2020.

[3] Q. Hao, S. Jufeng, and H. Pingming, "Study on dynamic characteristics and seismic response of the extradosed cable-stayed bridge with single pylon and single cable plane," *J Civil Struct Health Monit*, vol. 7, no. 5, pp. 589–599, 2017.

[4] W. Xie, L. Sun, and M. Lou, "Wave-passage effects on seismic responses of pile-soil-cable-stayed bridge model under longitudinal non-uniform excitation: shaking table tests and numerical simulations," *Bulletin of Earthquake Engineering*, vol. 18, no. 11, pp. 5221–5246, 2020.

[5] M. Xiong, Y. Huang, and Q. Zhao, "Effect of travelling waves on stochastic seismic response and dynamic reliability of a long-span bridge on soft soil," *Bulletin of Earthquake Engineering*, vol. 16, no. 9, pp. 3721–3738, 2018.

[6] E. Efthymiou and A. Camara, "Effect of spatial variability of earthquakes on cable-stayed bridges," *Procedia Engineering*, vol. 199, pp. 2949–2954, 2017.

[7] Z. Wang, L. Sun, and W. Cheng, "Analysis of seismic traveling wave effect of super long-span cable-stayed bridge," *Journal of Tongji University*, vol. 44, no. 10, pp. 1471–1481, 2016.

[8] L. Li, S. Hu, and L. Wang, "Seismic fragility assessment of a multi-span cable-stayed bridge with tall piers," *Bulletin of Earthquake Engineering*, vol. 15, no. 9, pp. 3727–3745, 2017.

[9] X. Yan, C. Cunyu, Z. Zeng, and Z. Shijie, "Shake table experimental study of cable-stayed bridges with two different design strategies of H-shaped towers," *Earthquake Engineering and Engineering Vibration*, vol. 20, no. 2, pp. 483–493, 2021.

[10] Z. Tonyali, S. Ates, and S. Adanur, "Spatially variable effects on seismic response of the cable-stayed bridges considering local soil site conditions," *Structural Engineering & Mechanics*, vol. 70, no. 2, pp. 143–152, 2019.

[11] Ş. Ateş, Z. Tonyali, K. Soyluk, and A. M. S. Samberou, "Effectiveness of soil-structure interaction and dynamic characteristics on cable-stayed bridges subjected to multiple support excitation," *Int J Steel Struct*, vol. 18, no. 2, pp. 554–568, 2018.

[12] M. Seeram and Y. Manohar, "Two-dimensional analysis of cable-stayed bridge under wave loading," *J. Inst. Eng. India Ser. A*, vol. 99, no. 2, pp. 351–357, 2018.

[13] A. G. Özcebe, C. Smerzini, and V. Bhanu, "Insights into the effect of spatial variability of recorded earthquake ground motion on the response of a bridge structure," *Journal of Earthquake Engineering*, vol. 24, no. 6, pp. 920–946, 2020.

[14] P. Clemente, G. Bongiovanni, G. Buffarini, and F. Saitta, "Structural health status assessment of a cable-stayed bridge by means of experimental vibration analysis," *J Civil Struct Health Monit*, vol. 9, no. 5, pp. 655–669, 2019.

[15] Zh. Zhu, W. Gong, K. Wang, Y. Liu, M. T. Davidson, and Lz Jiang, "Dynamic effect of heavy-haul train on seismic response of railway cable-stayed bridge," *J. Cent. South Univ.*vol. 27, no. 7, pp. 1939–1955, 2020.

[16] N. Jiantao, D. Yang, S. Yundong, and L. Zhongxian, "A simplified design method for metallic dampers used in the transverse direction of cable-stayed bridges," *Earthquake Engineering and Engineering Vibration*, vol. 19, no. 2, pp. 483–497, 2020.

[17] D. Mu, SG. Gwon, and D. H. Choi, "Dynamic responses of a cable-stayed bridge under a high-speed train with random track irregularities and a vertical seismic load," *Int J Steel Struct*, vol. 16, no. 4, pp. 1339–1354, 2016.

[18] O. Mouloud, T. Boualem, and H. Malek, "Effect of spatial variability of ground motion on non-linear dynamic behavior of cable stayed bridges," *MATEC Web of Conferences*, vol. 14902044 pages, 2018.

[19] J. Zhong, T. Yang, Y. Pang, and W. Yuan, "A novel structure-pulse coupled model for quantifying the column ductility demand under pulse-like GMs," *Journal of Earthquake Engineering*, vol. 25, pp. 1–19, 2021.

[20] J. Zhong, M. Ni, H. Hu, W. Yuan, H. Yuan, and Y. Pang, "Uncoupled multivariate power models for estimating performance-based seismic damage states of column curvature ductility," *Structures*, vol. 36, pp. 752–764, 2022.

[21] Q. Z. Tang, J. Z. Xin, Y. Jiang, J. Zhou, S. Li, and Z. Chen, "Novel identification technique of moving loads using the random response power spectral density and deep transfer learning," *Measurement*, vol. 195, no. 12, Article ID 111120, 2022.

[22] J. Z. Xin, Y. Jiang, J. T. Zhou, L. Peng, S. Liu, and Q Tang, "Bridge deformation prediction based on SHM data using improved VMD and conditional KDE," *Engineering Structures*, vol. 261, Article ID 114285, 2022.

[23] Q. Z. Tang, J. Z. Xin, Y. Jiang, J. Zhou, S. Li, and L Fu, "Fast identification of random loads using the transmissibility of power spectral density and improved adaptive multiplicative regularization," *Journal of Sound and Vibration*, vol. 534, Article ID 117033, 2022.

[24] Y. Zeng, Y. Zeng, and H. Yu, "Dynamic characteristics of a double-pylon cable-stayed bridge with steel truss girder and single-cable plane," *Advances in Civil Engineering*, vol. 2021, Article ID 9565730, 15 pages, 2021.

[25] Y. Zeng, Yu Qu, Y. Tan, Y. Jiang, and A Gu, "Analysis of fatigue cracking of orthotropic steel decks using XFEM," *Engineering Failure Analysis*, vol. 140, Article ID 106536, 2022.

[26] Y. Zeng, H. Zheng, Y. Jiang, J. Ran, and X He, "Modal analysis of a steel truss girder cable-stayed bridge with single tower and single cable plane," *Applied Sciences*, vol. 12, no. 15, p. 7627, 2022.

[27] C. Cui, R. Ma, and E Martinez-Paneda, "A phase field formulation for dissolution-driven stress corrosion cracking," *Journal of the Mechanics and Physics of Solids*, vol. 147, Article ID 104254, 2021.